Adv. Space Res. Vol. 9, No. 3, pp. (3)181–(3)190, 1989
Printed in Great Britain.

0273–1177/89 $0.00 + .50

GROUND-BASED MEASUREMENTS OF O^1D AND THE H_2O PRODUCTION RATE FROM COMETS

R. B. Kerr,* J. Bishop,** C. A. Tepley,*** S. K. Atreya,** R. P. Cageao,** I. M. Cherchneff** and T. M. Donahue**

**Center for Space Physics and The Department of Astronomy, Boston University, Boston, MA 02215 U.S.A.*
***Department of Atmospheric, Oceanic and Space Sciences, The University of Michigan, Ann Arbor, MI 48109, U.S.A.*
****Arecibo Observatory, Cornell University, P.O. Box 995, Arecibo, PR 00613, U.S.A.*

ABSTRACT

Ground-based high spectral resolution measurements of Comet Halley in the 6300.3 Å spectral region establish this technique as a powerful and low cost method for determining cometary H_2O production rates. A model of the line profile to be expected from the O^1D coma emission indicates that ground-based observations with fields of view on the comet of about 1×10^5 km measure profiles characteristic of O^1D from the H_2O parent. As the field of view increases, the signature of more energetic O^1D ejected by CO_2 and CO photolysis may become evident in the wings of the 6300.3 Å line profile. The width of the 6300.3 Å O^1D profile is found to be equal to the ejection speed of O^1D following H_2O phototolysis for fields of view to 1×10^6 km. Halley observations show that cometary NH_2 (0,8,0) emissions do not contaminate the cometary O^1D signature when the spectral resolution is $\leq$ 0.2 Å. H_2O production rates determined by scaling the measured O^1D production rates according to the H_2O photolysis branching ratio are in good agreement with other measurements. Minor upgrades in the tracking and spectral resolution capabilities of observatories now dedicated to measurements of the terrestrial airglow would be useful for expansion of the high resolution cometary O^1D data base – to include comets that come with less fanfare than did Halley.

INTRODUCTION

A bright cometary 6300 Å emission was first reported in 1958 by Swings and Greenstein /1/ in their analysis of Comet Mrkos. Due to the brightness of the emission, Bierman and Treffetz /2/ concluded that the emission could not be due entirely to fluorescence, and that a large population of metastable O^1D was being created by photodissociation of a parent molecule. Since that assertion there have been many attempts to determine the population of parent species based on available red line data (both 6300 Å and 6364 Å) and photochemical models. Excellent reviews appear in /3,4,5/.

Measurement of the 6300.3 Å intensity with sufficient accuracy to determine parent production rates based on photochemical models depends critically on treatment of spectral contamination. Terrestrial emissions can be isolated by the cometary Doppler shift with modest spectral resolution, but separation of cometary NH_2 (0,8,0) band emissions from the 6300.3 Å line requires spectral resolution of about 0.2 Å or better /6,7/.

The performance leader in high spectral resolution spectroscopy of cometary atmospheres is the group at the University of Wisconsin /6,8,9.10,11,12/. Using their twin-etalon Fabry-Perot spectrometer attached to the 0.81 m McMath solar telescope at Kitt Peak Arizona, the first spectrum of the 6300.3 Å cometary line isolated from both the terrestrial red line and cometary NH_2 emissions was published in 1975 /6/. During the Halley apparition, the Wisconsin system was used to image the red line from 8.0×10^3 km from the nucleus outward to about 8×10^4 km free from spectral contamination /11,12/. The Wisconsin spatial imaging study of 6300.3 Å intensity concludes that the dominant source of O^1D emission within about 1×10^5 km of the nucleus is due to O^1D from H_2O photodissociation. This result validates determination of the water production rate, $Q(H_2O)$, from the O^1D production rate, $Q(O^1D)$, for fields of view $< 1 \times 10^5$ km centered on the comet nucleus. The calculation must also account for metastable decay beyond the field of view, and collisional quenching near the nucleus.

This paper models the high spectral resolution 6300.3 Å line profiles to determine the relative contributions to the emission that can be expected from the distinct O^1D daughters produced by photodissociation H_2O, CO_2, and CO. The model results are compared with profiles measured with a much more modest system than

that used by Wisconsin - a single etalon Fabry-Perot interferometer interfaced with a commercially available 0.4 m telescope. The sources of metastable O^1D atoms in cometary comae include:

$$H_2O + h\nu \rightarrow H_2 + O^1D \quad (1)$$
$$\rightarrow OH + H \quad (2)$$
$$OH + h\nu \rightarrow H + O^1D \quad (3)$$
$$CO + h\nu \rightarrow C + O^1D \quad (4)$$
$$CO_2 + h\nu \rightarrow CO + O^1D \quad (5)$$

/3,13,14/.

COMETARY LINE PROFILES

Here we discuss the line profile to be expected in $O(^1D)$ 6300.3 Å coma emissions, in particular in ground-based observing situations when the field of view (FOV) is centered on the nucleus and the radius of the field of view (R_{FOV}) is large compared to nuclear dimensions. We neglect variation of parent photodissociation rates within the coma and, except for the imposition of a dust zone centered on the nucleus, we ignore attenuation of 6300.3 Å photons.

In keeping with this assumed observing scheme, a velocity space described in terms of cylindrical coordinates (v_s, v_t, ϵ) is joined to each coma location **r** specified by spherical coordinates (r, θ, ϕ) centered on the nucleus. Here, v_s is the component of the constituent velocity along the line of sight (LOS) in a reference frame moving with the nucleus, v_t is the component transverse to LOS, r is the distance from the nucleus, θ is the angle between **r** and the observer-nucleus axis, ϕ is the azimuth about this axis, and ϵ is the azimuth about the LOS through **r** (ϕ and ϵ share reference planes). These coordinates are illustrated in Figure 1.

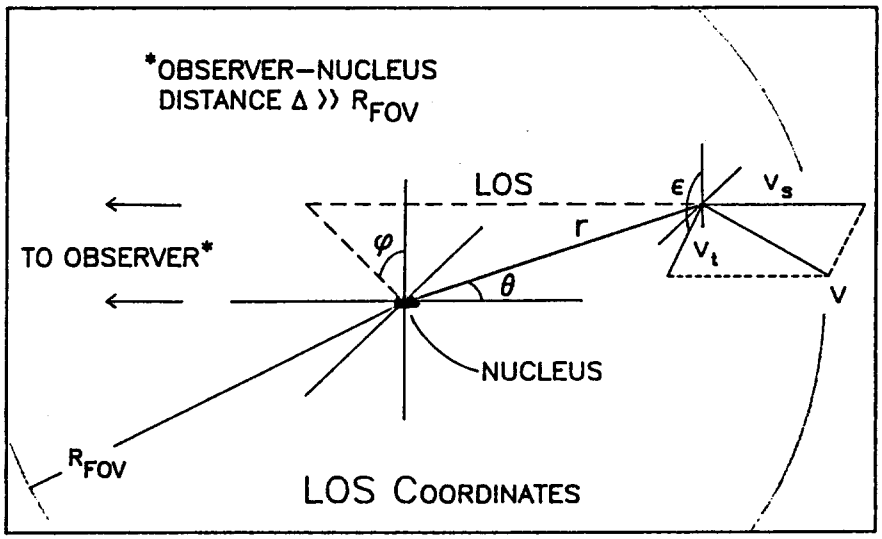

Fig. 1. LOS geometry.

In terms of the kinetic distribution f for the metastable species, the spectral profile for this geometry is

$$\frac{4\pi\tau_d}{\gamma} I(v_s) = \int_{-1}^{1} d\mu \int_{R_L}^{R_{FOV}\cdot\sin\theta} dr\, r^2 \int_0^{2\pi} d\omega \int_0^{\infty} dv_t\, v_t \int_0^{2\pi} d\epsilon\, f \quad (6)$$

where τ_d is the net lifetime of the metastable upper state and γ is the branching ratio when the decay is into multiple lower states (for $O(^1D)$ 6300.3 Å observations, this ratio is 3/4). The multiple integral on the RHS gives the total number of metastable atoms within the observed coma with the specified LOS velocity v_s. The lower radial limit R_L can usually be set to zero, though it is no real complication to include screening; specifically, if R_o denotes the radius of a presumed spherical zone of optical thickness greater than unity (established by dust), then

$$R_L = \begin{cases} R_o, & v_s < 0 \\ R_o/\sin\theta, & v_s \geq 0 \end{cases}$$

Now to specify f. Often considerable excess energy remains to be distributed among the molecular fragments following photodissociation. For example, Huebner's revised estimates for excess energies in the generation of $O(^1D)$ from likely primary parent molecules lead to the "ejection" speeds given in Table 1 /14/. Compared with typical thermal speeds (0.5 km sec^{-1} for atomic oxygen at $T_g \approx 200°K$), the motion of the emitting species can be dominated by the excess energy deriving from photodissociation. By assuming the daughter metastable atoms are monoenergetic and ejected isotropically in the local rest frame, a coma line profile is easily constructed for photodissociative production; this is basically the "vectorial" approach of Festou /13/ and as presented here is valid when H_2O or OH is the parent, since $O(^1D)$ then results primarily from absorption of solar Lyman-α /15,16/.

TABLE 1 $O(^1D)$ Parents

SPECIES	TOTAL LIFETIME* (sec)	BRANCHING RATIO**	"EJECTION" SPEED (km sec^{-1})
H_2O	8.33×10^4	0.12	2.07
OH***	1.17×10^5	0.05	1.60
CO	1.54×10^6	0.065	5.57
CO_2	5.00×10^5	0.46	5.74

* At 1.0 AU
** Assuming excess energy channeled only into kinetic energy of products
*** From /16/

For now, consider a single parent and consider the density of metastable atoms $n(r)$ at a coma location (r, θ, ϕ) as viewed in a frame of reference moving with the local flow of parent molecules. In this comoving frame, the monoenergetic, isotropic kinetic distribution in LOS cylindrical velocity coordinates is /17/

$$f = \frac{n(r)}{4\pi v_o} \cdot \frac{\delta(v_t - [v_o^2 - v_s^2]^{1/2})}{[v_o^2 - v_s^2]^{1/2}} \tag{7}$$

where v_o is the ejection speed of the metastable atom. Transforming to the comet nucleus rest frame, v_s is replaced by $v_s - \mu\dot{v}$, where $\dot{v}$ is the radial outflow speed of the parent gas from the nucleus and $\mu = \cos\theta$. Substituting into (1), the spectral profile becomes

$$\frac{4\pi\tau_d}{\gamma} I(v_s) = \frac{\pi}{v_o} \int_{\mu_L}^{\mu_U} d\mu \int_{R_L}^{R_{FOV}/\sin\theta} dr\, n(r) r^2 \tag{8}$$

where μ_U is equal to $(v_o + v_s)/\dot{v}$ or 1.0, whichever is smaller (if $\mu_U < -1.0$, the entire integral is set to zero). Similarly, μ_L is the larger of $-(v_o - v_s)/\dot{v}$ or -1.0, the entire integral being zero if $\mu_L > 1.0$.

The density of the observed species $n(r)$ is easily prescribed in the steady state once the parent density distributions are known, since the metastable decay occurs in the vicinity of the parent's photodestruction:

$$\frac{n(O(^1D))}{\tau_d} = \frac{\beta_1 n_1}{\tau_{g_1}} + \frac{\beta_2 n_2}{\tau_{g_2}} + \cdots \tag{9}$$

where the summation extends over parent species, τ_{g_i} is the lifetime of the parent, and β_i is the branching ratio for $O(^1D)$ production. For a single parent coming directly from the nucleus, the Haser "parent" distribution/18/ can be used to obtain

$$\frac{4\pi\tau_d}{\gamma} I(v_s) = \frac{\beta Q_p \tau_d}{4v_o} \int_{\mu_L}^{\mu_U} d\mu \left\{ \exp\left[\frac{(R_L - R_o)}{\dot{v}\tau_g}\right] - \exp\left[-\frac{(R_{FOV}/(1-\mu^2)^{1/2} - R_o)}{\dot{v}\tau_g}\right] \right\} \tag{10}$$

where Q_p is the rate of sublimation of the parent molecule from the nucleus.

The most interesting aspect of these profiles is the dependence on coma outflow speed $\dot{v}$. Figure 2a shows a profile using nominal Halley parameter values at about the time of the spacecraft encounters with H_2O as the sole parent and $\dot{v} = 0.9$ km sec^{-1}; Figure 2b was generated with $\dot{v} = 1.2$ km sec^{-1}. Due to photolytic heating

in the coma, the outflow speed is not constant but actually increases to an asymptotic value/18,19/; the values used in Figure 2 are suggested by Giotto NMS measurements/20/. Since most $O(^1D)$ generation occurs well out from the nucleus, this asymptotic outflow speed is the one most appropriate for use in interpreting 6300.3 Å line profiles obtained with large fields of view.

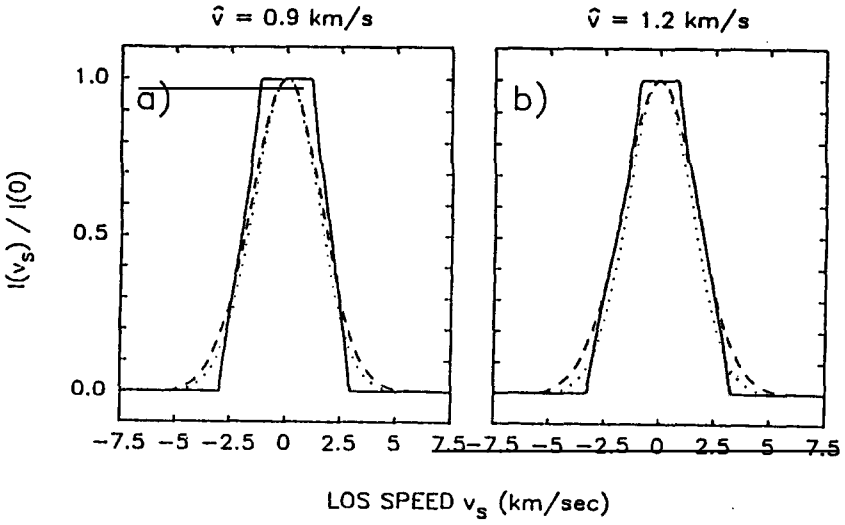

Fig. 2. a) $O(^1D)$ profile given by Eqn. (5) (solid curve), using H_2O parameter values 1.15cm of Table 1 and $\hat{v}$ = 0.9 km sec^{-1}. The Gaussian profile (dotted curve) is generated with the H_2O ejection speed given in Table 1, while the dashed curve is exp[$-v_s^2/(v_o^2(H_2O) + \hat{v}^2)$]. 1.15cm b) Same as panel a) but with $\hat{v}$ = 1.2 km sec^{-1}. In both panels, R_{FOV} = 10^5km.

There is also a dependence on observing geometry, illustrated in Figure 3a. In the limit of large R_{FOV} (entire molecular coma observed), the profiles are trapezoidal in shape; if R_{FOV} should be smaller than the scale length of the primary parent, the profile is artificially weighted in the wings (tunnel vision effect).

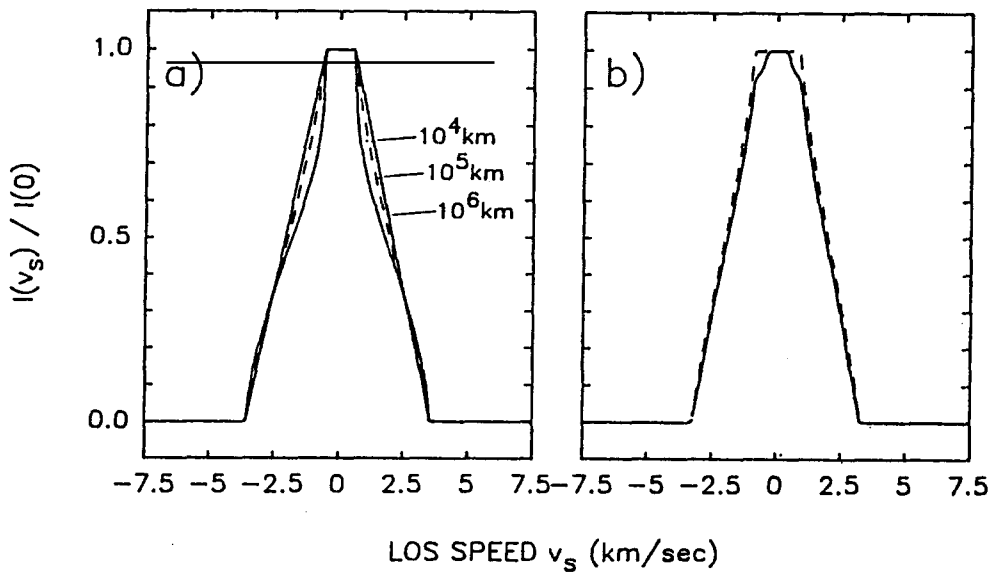

Fig. 3. a) Variation of profile with R_{FOV}. Choice of $\hat{v}$ = 1.5 km sec^{-1} was made to accentuate the effect. b) Effect of including OH source. Solid curve shows superposed contributions from H_2O and OH photodissociation, with OH modeled as a Haser "daughter" of H_2O. Dashed curve is profile for H_2O alone (same as solid curve from Figure 2b). R_{FOV} = 10^5km and $\hat{v}$ = 1.2 km sec^{-1}.

Contributions to the observed line from several parents can easily be modeled by superposing individual single parent lines. Contributions from CO and CO_2 would have been barely perceptible in Figure 2, not merely because of smaller sublimation rates but also because of the longer times for photo-generation of $O(^1D)$. After H_2O, the most significant $O(^1D)$ parent is OH. The distribution of OH in a cometary coma is not particularly well described by a Haser model (especially the kinetic distribution) and really requires the use of a full vectorial approach. However, to illustrate the effect of OH contributions to the line profile in a crude manner, Figure 3b shows the profile that results when OH is modeled as a Haser H_2O "daughter" species /18/, using the parameter values of Table 1. The profile modifications brought about by including OH are probably not observable with current instrumental limitations, since it is not as virile a parent as H_2O (most OH dissociations lead to production of $O(^3P)$) and the resulting ejection speed is not greatly different from the H_2O value. The OH contribution is best studied using imaging techniques /12/. In any event, observations with $R_{FOV} \leq 10^5$km will be dominated by the H_2O source.

It is of course necessary to take proper account of the emission profile when estimating total intensities or extracting ejection speeds, either of which requires deconvolving an instrument function from the observed profile. For instance, Huppler et al. /6/ extracted full widths at half-maximum (FWHM) of $\approx$ 2.7 km sec^{-1} from observations of $O(^1D)$ 6300.3 Å emissions from comet Kohoutek, narrower than expected on the basis of the development outlined above. This might be traceable to their assumption that the emission profile is Gaussian, or it may indicate that some aspect of the physics of $O(^1D)$ generation has gone unrecognized; before the latter can be invoked, the former must be explored. A similar caveat holds regarding the use of $O(^1D)$ 6300.3 Å intensity measurements to estimate H_2O production rates.

INSTRUMENTATION

Spectral line profiles of the 6300.3 Å emission from Comet Halley have been obtained using a single etalon Fabry-Perot interferometer interfaced to a 40.6 cm Newtonian telescope at the Arecibo Observatory. These observations were made post-perihelion, in March and April, 1986. A schematic drawing of the instrument configuration is shown in Figure 4.

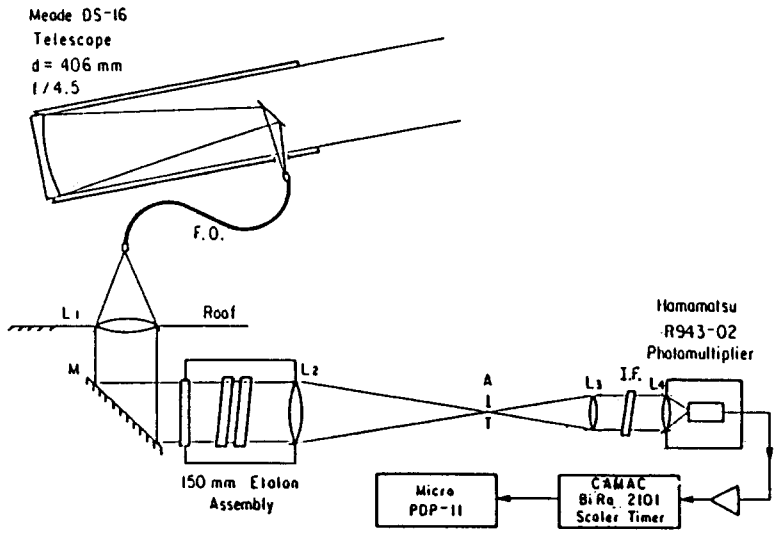

Fig. 4. Light from the comet is transmitted from the telescope to the FPI plates using a fiber optic light guide cable. Light exiting the cable is collimated using lens L1 with a focal length (f) of 63 cm. The collimated light then relects from the 45° mirror, M, to the etalon plates. The FPI interference pattern is then focused by the objective lens L2 (f=122 cm) to the pinhole aperture A. The light is then collimated by lens L3 (f=30 cm) prior to passing through the interference filter I.F. The light 1.15cm is then focused onto the photomultiplier tube by lens L4 (f=2.5 cm.)

The interferometer scans in wavelength by varying the pressure (and therefore refractive index) of SF_6 gas between the etalon plates. The free spectral range of the FPI is 1.80 Å (85.85 km s^{-1}) at 6300.3 Å. The FPI is operated at a finesse of about 10 for these observations, so the spectral resolution is about 8.6 km s^{-1}. The spectral band pass of the system is defined by the band pass of the interference filter. The interference filter used in this experiment is a three cavity filter, giving a nearly square bandpass 3.2 Å broad at the half transmission point.

Due to the possibility of cometary NH_2 and terrestrial OH contamination in the 6300.3 Å spectral region, it is important to understand the actual band pass of the system in this region. The throughput of the system is maximized while observing the 6300 Å terrestrial emission, so that the nominal band pass in the earth reference frame is 6300.3 ± 1.6 Å. However, small variations of the filter temperature can shift the bandpass, approximately 1 Å per 4° C. Although the filters are somewhat insulated from the ambient room atmosphere, we conservatively ascribe the room temperature variations to filter temperature variations. These variations were monitored, and found to be about ±2° C. We estimate that spectral features in the range 6300.3 ± 2.1 Å might be passed by the system. Features in this region appearing more than 0.9 Å (one half of a free spectral range) from the 6300.3 Å rest position will overlap into first free spectral range. For example, a feature at 6298.62 Å will appear in the first free spectral range at 6298.62 Å + 1.8Å = 6300.42 Å. A feature at 6297.9 Å (terrestrial OH emission) will not be passed by the system.

Absolute sensitivity calibration is achieved by cross calibration with a tilting filter photometer that is calibrated with a ^{14}C source. The FPI and photometer measure common volumes of the terrestrial 6300 Å emission for cross calibration. Of course, the width of the cometary emission feature is narrower than the terrestrial feature a factor of about 1.7, and the calibration must be adjusted accordingly.

OBSERVATIONS

Optical observations of Comet Halley at the Arecibo Observatory began in January, 1986, before perihelion. Instrumental and weather related difficulties limited useful data to the post-perihelion period in March and April, 1986. The field of view of the instrument was 5'.9, equivalent to approximately 2×10^5 km at the distance of the comet in March, and about 1.1×10^5 km in April. The apparition at Arecibo was characterized by low elevations during this period, never exceeding 30° during the available dark hours. The equatorial drive system of the telescope required periodic electronic correction, and we estimate the tracking accuracy to be about 2 arcsec min^{-1}. A typical scan of one free spectral range required about 12 minutes. The observation procedure has been detailed further in /21,22/, and these papers display data from the March, 1986 period.

Figure 5 shows four examples of the 6300 Å spectra obtained from Comet Halley in April 1986. Spectra from March 1986 are shown in /21,22/. The cometary O^1D emission is resolved from the terrestrial emission due to the motion of the comet in each case. Also, features on the long wavelength side of the cometary O^1D emission are evident in each panel, and the O^1D feature iteslf appears asymmetric on the red side. These features and the asymmetry are attributed to cometary NH_2 emissions.

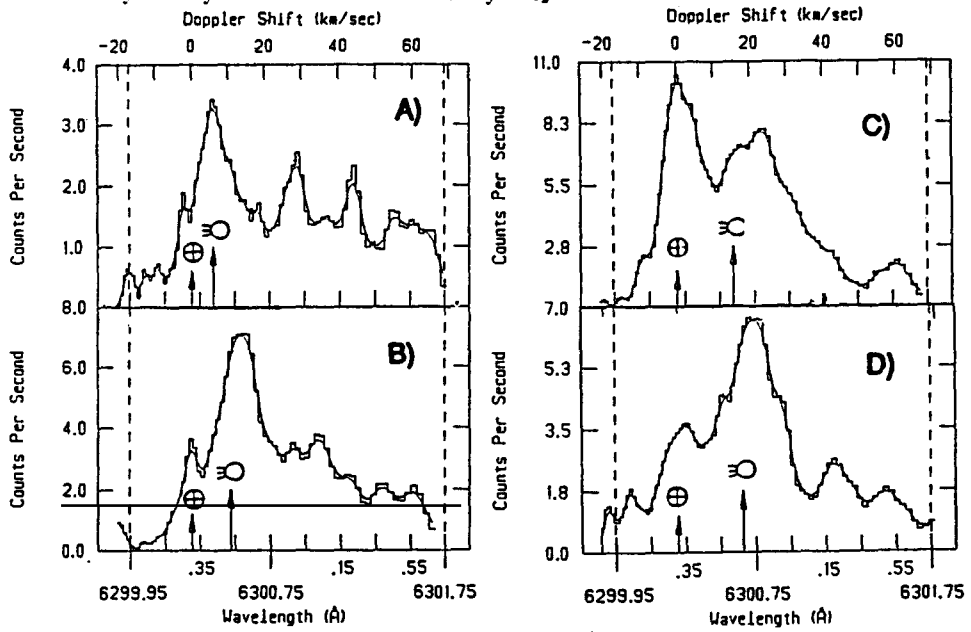

Fig. 5. Four examples of head centered scans of the 6300 Å region. The Doppler shift and wavelength scales on the upper and lower abscissas are for the earth reference frame. The vertical dashed lines define one free spectral range of the FPI. The 6300 Å earth rest position is denoted by an arrow pointed upward with the earth symbol above it. The arrow with the comet symbol above indicates the expected position of the cometary O^1D emission. a) 11 April 1986 1.70 UT. b) 12 April 1986 4.91 UT. c) 13 April 1986 6.67 UT. d) 14 April 1986. In each case two scans have been added for an effective I.P. of 20 s per point. Each full scan pf the spectral region requires about 14 minutes.

A persistent feature in our 6300.3 Å data appears approximately 0.49 Å to the red of the cometary O^1D emission. This emission can be attributed to either the NH_2 Q branch 3_{13} - 3_{02} (0,8,0) or 4_{14} - 4_{04} (0,8,0) emissions, at 6299.0 and 6300.8 Å in the cometary rest frame respectively /23/. The lower wavelength emission overlaps into the same region as the higher in the second order of the instrument band pass. No NH_2 emissions due to transitions in lower rotational levels can account for this feature. Attributing this NH_2 feature to population of the third or fourth rotational level is contrary to the results of /7,12/. However, the observations of /12/ were made before perihelion and again in late April 1986. Apparently, a measurement on 5 April 1988 did not reveal these higher rotational level emissions. The measurements of /7/ were also made in late April 1986. Other, less intense features further to the red might also be attributed to transitions in rotational levels above 3, but cannot be attributed to levels ≤ 3. Due to the weakness of these features and tracking difficulties, we eschew further comment on these weak features.

The red side asymmetry is due to the NH_2 2_{12} - 2_{02} (0,8,0) transition at 6298.6 Å appearing at 6300.4 Å in the second order of the band pass. The second member of this doublet is not within the filter band pass. Due to this NH_2 contamination very near to cometary O^1D emission, a crude estimate of the 6300.3 Å intensity is made here by fitting to the peak of the cometary emission. The instrument sensitivity at this wavelength is 0.10 counts s^{-1} R^{-1} ± 30%.

RESULTS AND DISCUSSION

The measured intensities and derived production rates of O^1D are shown in Table 2. The production rate of O^1D is estimated by

$$Q_{O^1D} \simeq (\frac{4}{3}) 4\pi \Delta^2 \Omega I_{6300} \tag{11}$$

where 4/3 accounts for decay channel of O^1D giving the 6364 Å emission. Δ is distance from the observer to the comet and Ω is the solid angle of the FPI field of view. This ignores quenching of O^1D in the collisional zone near the nucleus and the production of O^1D by H_2O beyond the field of view. For these fields of view, on the order of $1\text{-}2\times10^5$ km, quenching is entirely negligible /3/. Metastable creation beyond this field of view depends upon the lifetime of parent species against dissociation, which increases as the square of heliocentric distance /12/, and upon the size of the field of view at the comet distance. For these reasons, Q_{O^1D} must be adjusted upward by a factor of about 1.65 in April, while a negligible amount of metastable decay occurs beyond the field of view for the March geometry.

Although the effects of OH photolysis on the 6300 Å line profile are small for these fields of view, OH photolysis must be considered when attempting to derive the water production rate from 6300.3 Å emission /12/. The water production rates in Table 2 are calculated by multiplying the O^1D production rates by seven, in line with the work of /12/ and the theoretical brancing ratios in Table 1. /12,14,16/. Errors listed in Table 2 are root mean squares of all spectra analyzed for a certain night, and the intensities have been adjusted for extinction by interploating the results of /8/.

TABLE 2 6300 Å Intensity, O^1D and H_2O Production Rates

Date	* R_o (A.U.)	Intensity (Rayleighs)	Q_{O^1D} (sec^{-1})	Q_{H_2O} (sec^{-1})
15 March	0.92	156±32	$1.2 \pm 0.5 \times 10^{30}$	$8.4 \pm 1.8 \times 10^{29}$
17 March	0.94	185±20	$1.1 \pm 0.1 \times 10^{29}$	$7.7 \pm 0.8 \times 10^{29}$
11 April	1.35	37±11	$3.1 \pm 1.8 \times 10^{28}$	$2.2 \pm 1.0 \times 10^{29}$
12 April	1.37	72±22	$5.9 \pm 1.8 \times 10^{28}$	$4.1 \pm 1.0 \times 10^{29}$
13 April	1.38	90±30	$7.2 \pm 2.2 \times 10^{28}$	$5.0 \pm 1.6 \times 10^{29}$

* heliocentric distance

In Figure 6 we compare a measured O^1D line profile with a theoretical profile. The theoretical profile includes the NH_2 2_{12} - 2_{02} (0,8,0) emission line with an intensity similar to that reported by /12/. This profile is convolved with the FPI instrumental function that is measured with a frequency stabilized He-Ne laser. The theoretical profile assumes an outflow velocity, v_s, of 1.2 km s^{-1}. Although OH may be an important parent of O^1D with this field of view, the O^1D ejection velocity from OH photolysis does not greatly effect the shape of the theoretical profile.

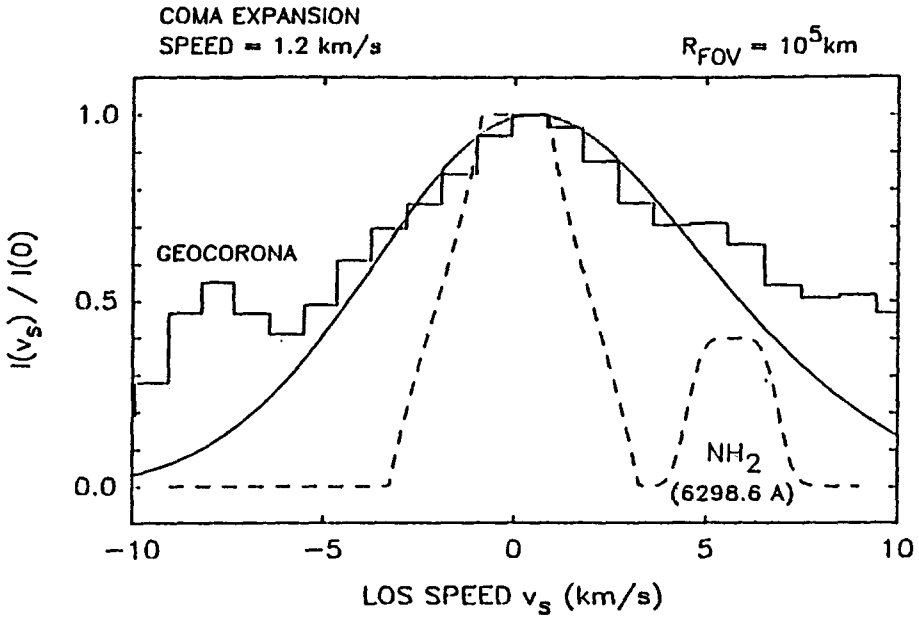

Fig. 6. The profile of Figure 5a has been normalized to unity at the peak count rate and compared to theoretical profile generated with equation 10. A field of view of 10^5 km has been used in the theoretical calculation, very near to that used for the observation. Additional explanation appears in the text.

CONCLUSIONS

High spectral resolution observations of the 6300 Å line profile are a powerful and simple diagnostic for the study of cometary comae. The line profile must be known to accurately calculate Q_{O^1D} using the 6300.3 Å intensity. Also, the theoretical profiles show the outflow velocity of the parent molecules from the nucleus can be determined using the FPI observations. This technique will prove particularly useful for comets that appear suddenly relative to the time required to schedule major experiments.

This particular experiment can be improved in several ways to prepare for future apparitions. Some of the most important changes include:

The interference filter should be as narrow as possible when using the single etalon Fabry-Perot configuration. The narrow band pass serves to limit the extent of inter-order overlap that can contaminate the first free spectral range.

The interference filter should be strictly temperature stabilized to prevent drift from broadening the effective band pass.

Telescope tracking and seeing conditions probably require image grade fiber optic cable be used. This would prevent large oscillations of background signals due to irregular illumination at the end of fiber bundles.

Observations with fields of view well under 10^5 km should be interleafed with fields of view well in excess of 10^5 km to investigate carefully the branching ratios and ejection speeds of water and OH photolysis, as well as outflow velocity of the parent species.

ACKNOWLEDGMENTS

We would like to thank F. Roesler for numerous enlightening conversations on several points covered in this paper. The Arecibo Observatory is operated by Cornell University under contract with the National Science Foundation. This research was supported grants NSG-7404 from the NASA/Planetary Atmospheres program, and NASA grant NAS2-12314.

REFERENCES

1. P. Swings and J. L. Greenstein, Présence des raies interdites de l' oxygène dans les comètes, *Comptes Rendus Acad. Sci., Paris,* **246**, 511 (1958)

2. L. Biermann and E. Trefftz, Ueber die mechanism der ionisation and der anregung in kometenatmospheren, *Z. Astrophys.,* **59**, 1 (1964)

3. M. C. Festou and P. D. Feldman, The forbidden oxygen lines in comets, *Astron. Astrophys.,* **103**, 154 (1981)

4. H. Spinrad, Observations of the red auroral lines in nine comets, *Astron. Soc. Pacific,* **94**, 1008 (1982)

5. A. H. Delsemme, What we do not know about cometary ices: A review of the incomplete evidence, in: Ices in the Solar System, ed. J. KAlinger *et al.,* D. Reidel Publ. Co., 1985, p. 505.

6. D. Huppler, R.J. Reynolds, F.L. Roesler, F. Scherb, and J. Trauger, Observations of Comet Kohoutek (1973f) with a ground-based Fabry-Perot spectrometer, *Astrophys. J.* **202**, 276 (1975)

7. C. Arpigny, P. Magain, J. Manfroid, F. Dossin, A. C. Danks, and D. L. Lambert, Resolution of the [OI] + NH_2 blend in comet P/Halley, *Astron. and Astrophys.,* **187**, 485 (1987)

8. F. Scherb, Hydrogen production rates from ground-based Fabry-Perot observations of Comet Kohoutek, *Astrophys. J.,* **243**, (1981)

9. P. Shih, F. Scherb, and F. L. Roesler, Hydrogen production rate from Comet Austin 1982g, *Astrophys. J.,* **299**, 453 (1984)

10. F. Scherb, F. L. Roesler, K. Magee, J. Harlander, and R. J. Reynolds, Fabry-Perot ground-based observations of Comet Halley, *Adv. Space Res.,* **5**, # 12, 275 (1985)

11. F. L. Roesler, F. Scherb, K. Magee, J. Harlander, R. J. Reynolds, R. V. Yelle, A. L. Broadfoot, and R. J. Oliversen, High spectral resolution line profiles and images of Comet Halley, *Adv. Space Res.,* **5**, # 12, 279 (1985)

12. K. P. Magee-Sauer, Ground-based Fabry-Perot observations of neutral and ionic atoms and molecules of Comet Halley, Dissertation, University of Wisconsin (1988)

13. M. C. Festou, The density distribution of neutral compounds in cometary atmospheres, *Astron. Astrophys.* **95**, 69 (1981)

14. W. F. Huebner, The photochemistry of comets, in: The Photochemistry of Atmospheres, J.S. Levine, ed., Academic Press, Orlando, 1985.

15. J. Crovisier, Note on the photodissociation of water in cometary atmospheres: Implications for the water lifetime, the kinematics of H and OH, photolytic heating of the coma and infrared emission of OH, unpublished manuscript (1988)

16. E. F. van Dishoek and A. Dalgarno, The dissociation of OH and OD in comets by solar radiation, *Icarus* **59**, 305 (1984)

17. J. Bishop and S.K. Atreya, Cometary line profiles, unpublished manuscript (1988)

18. see. for instance, Mendis, D.A., H.L.F. Houpis, and M.L. Marconi, The physics of comets, *Funda. Cosmic Phys.* **10**, 1 (1985)

19. M. R. Combi and W.H. Smyth, Monte Carlo particle trajectory models for neutral cometary gases I. Models and equations, *Astrophys. J.* **327**, 1026 (1988)

20. P. Lammerzahl, D. Krankowsky, R.R. Hodges, U. Stubbemann, J. Woweries, I. Herrwerth, J.J. Berthelier, J.M. Illiano, P. Eberhardt, U. Dolder, W. Schulte, and J.H. Hoffman, Expansion velocity and temperatures of gas and ions measured in the coma of comet P/Halley, *Astron. Astrophys.* **187**, 169 (1987)

21. R. B. Kerr, R. P. Cageao, C. A. Tepley, S. K. Atreya, and T. M. Donahue, High spectral resolution Fabry-Perot measurements of Comet Halley at H-alpha and 6300 Å, *Adv. Space Res.*, **5**, # 12, 283 (1986)

22. R. B. Kerr, C. A. Tepley, R. P. Cageao, S. K. Atreya, T. M. Donahue, and I. M. Cherchneff, Observations of Comet Halley at H_α and 6300 Å, *Geophys. Res. Lett.*, **14**, 53 (1987)

23. K. Dressler and D. A. Ramsay, The electronic absorption spectra of NH_2 and ND_2, *Phil. Trans. R. Soc. Lond. A*, **251**, 553 (1959)

24. H. Lew, Electronic spectrum of H_2O^+, *Can. J. Phys.*, **54**, 2028 (1976)

25. R. R. Meier, Resonance scattering from optically thin expanding cometary atmospheres, *Astron. Astrophys.*, **40**, (1975)